PHYSICAL REVIEW B VOLUME 57, NUMBER 12 15 MARCH 1998-II

Reinvestigation of the Ni/Si interface: Spectromicroscopic evidence for multiple silicide phases

L. Gregoratti, S. Günther, J. Kovac,* L. Casalis, M. Marsi, and M. Kiskinova
Sincrotrone Trieste, Area Science Park, I-34012 Trieste, Italy

(Received 8 December 1997)

Using photoelectron spectromicroscopy we identified the chemical composition of several phases on a morphologically complex interface formed after segregation of dissolved Ni onto the Si(111) surface. Unexpectedly, coexistence of two types of micrometer-sized silicide islands with composition and electronic structure close to $NiSi_2$ and NiSi phases was found. This finding revises some of the previous schemes about the evolution of the Ni/Si(111) system at high temperatures, which were based exclusively on structural analyses. A formation mechanism supposing anisotropy of the nucleation barrier for disilicide formation is suggested in order to explain the presence of NiSi islands and the preferred $\langle 110 \rangle$ orientation of the $NiSi_2$ islands. [S0163-1829(98)52612-4]

Ni silicide films grown on Si substrates are among the most extensively studied metal silicide systems because of their wide application as ohmic contacts in Si-based technology. Many ordered surface and bulk phases of different structure and composition, which grow nearly epitaxially on the Si substrate, have been reported.[1] Recently, much of the academic effort was focused on the initial stages of silicide formation via solid phase epitaxy (SPE), the mechanism of Ni mass transport, and the formation conditions and atomic arrangements of the $\sqrt{19}\times\sqrt{19}$ and ''1×1''-ring cluster (RC) surface reconstructions at submonolayer Ni coverages.[1–6] The general agreement about the reactions sequence during SPE is that $NiSi_2$ should be the only phase remaining after annealing of deposited thin Ni films to ~1070 K.[1] Because of the high solubility of Ni in Si at temperatures >1000 K it is believed that the bulk interstitial diffusion is the dominant mass transport for Ni, which is the main diffusing species.[1,2] The precipitation of dissolved Ni can result in formation of ordered $\sqrt{19}$ and ''1×1''-RC surface phases, when the Ni coverages are less than ~0.15 ML, and growth of three-dimensional (3D) islands at coverages above 0.15 ML.[1] Structural techniques [reflective high-energy electron diffraction (RHEED), low energy electron microscopy (LEEM), and scanning electron microscopy (SEM)] have identified the 3D islands as a $NiSi_2$ phase which is consistent with the high formation temperatures used.[3–6]

Using the recently developed synchrotron radiation scanning photoelectron microscopy we reinvestigated the lateral distribution and composition of the phases formed when one monolayer of Ni dissolved in Si segregates onto the surface. Thanks to the capability of the scanning photoemission microscope (SPEM) to probe the interface chemical composition and structure with submicron spatial resolution we identified two kinds of 3D silicide islands different in shape and orientation, each one with different composition and electronic structure. These results reveal new aspects of the interface reactions occurring during Ni segregation which question the general validity of the accepted scheme for the evolution of the silicide phases produced by SPE.

The experiments were carried out with the scanning photoemission microscope (SPEM) on the ESCA microscopy beamline at the ELETTRA light source. The SPEM used photon focusing optics for demagnification of the beam to a spot with a diameter of $\leqslant 0.15$ μm. Specific information about the composition and electronic structure of the Ni/Si interface is provided by collecting and analyzing the photoelectrons (PE) emitted from the irradiated area using a hemispherical electron analyzer. In order to get spatially resolved chemical maps, the collection of emitted core level photoelectrons was synchronized by scanning the sample with respect to the focused beam. A more detailed description of the beamline and SPEM setup and the UHV-connected preparation chamber equipped with low-energy electron diffraction (LEED) and Auger electron spectroscopy (AES) analyzers can be found in Ref. 7.

In the present study, we used 490 eV photons which allowed us to monitor the Si $2p$, Ni $3p$, and valence band photoelectrons with sufficient photoelectron yield and energy resolution. The Si $2p$ spectra were fitted using a curve fitting procedure of Doniach-Sunjic convoluted with Gaussian for the instrument resolution (0.4 eV in the present measurements).[7] As a reference, the binding energy (BE) position and parameters of the bulk Si component from the fit of the Si $2p$ spectrum measured by us for the Si(111)-7×7 sample, was used. For coverage calibration of the deposited Ni we used the Si $2p$ and Ni $3p$ PE and Si(KLL) and Ni(LMM) Auger intensities measured for the $\sqrt{19}$ compressed structure containing ~0.16 ML of Ni.[3] 1 ML equals the number of Si surface atoms on Si(111)-1×1, 7.83×10^{14} atoms/cm^2. The Si(111)-7×7 surface was prepared by the usual controlled flashing procedures using direct resistive heating.[8] The interface was produced by room temperature deposition of a total of 1 ML Ni (with a rate of 0.05 ML/min) in doses of ~0.25 ML. After each deposition step the sample was annealed for 15 sec at 1150 K (well above the solvus line) cooled down and kept at 920 K for ~45 sec (below the solvus line), followed by slow cooling (~1.5 K/sec) to room temperature. This procedure reportedly created a ''1×1''-RC phase and 3D $NiSi_2$ islands.[3,6] Our LEED data showed very weak 7×7 and more intense (1×1) spots in accordance with the above reported ''1×1''-RC phase which usually coexists with 7×7 Si domains.

Figure 1 shows a typical chemical map of the Ni/Si system obtained by collecting the Ni $3p$ photoelectrons. The

 © 1998 The American Physical Society

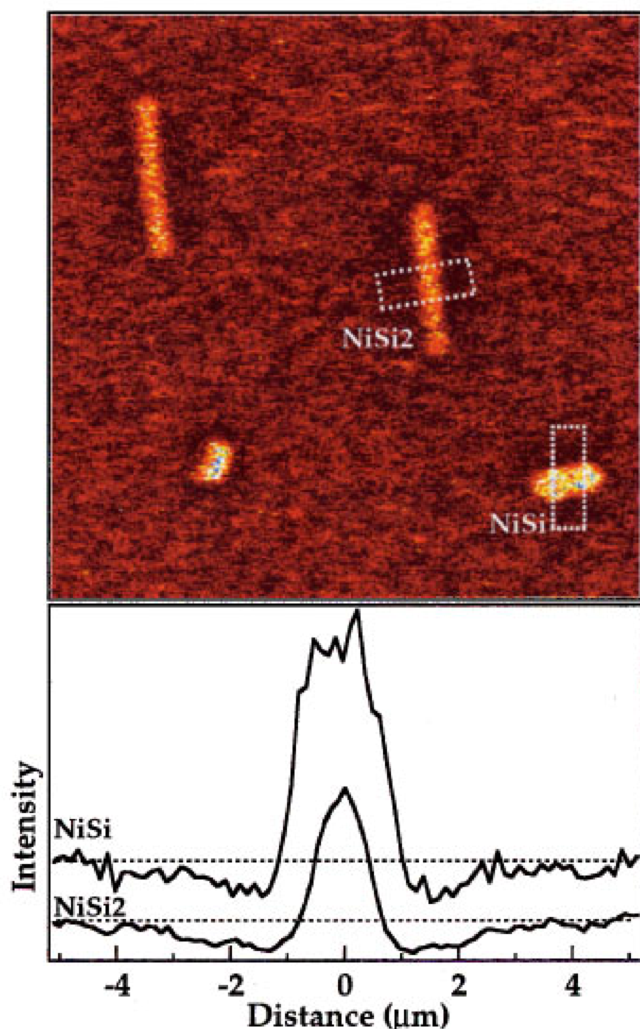

FIG. 1. (Color) Ni $3p$ map (top) and profile linescans (bottom) across the 3D islands averaged over the indicated area in the map.

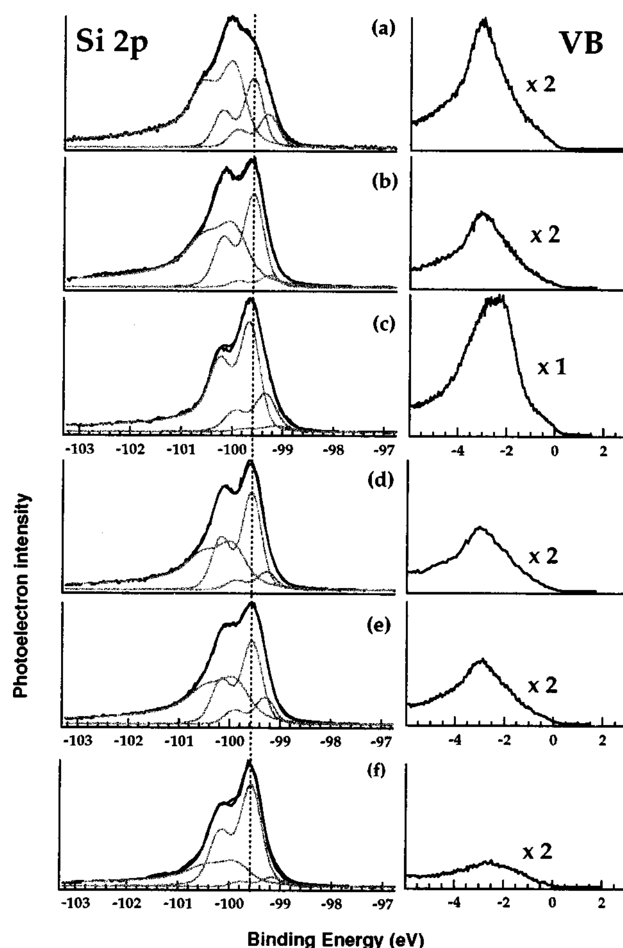

FIG. 2. Si $2p$ and valence band (VB) spectra taken from: (a) and (b) $NiSi_2$ islands with different thicknesses of the Si cap; (c) NiSi-like island; (d) and (e) brighter and darker out-of-island regions; (f) the depletion zone surrounding the islands. The fitting components of Si $2p$ spectra are presented by grey lines. The dashed line indicates the Si $2p_{3/2}$ BE of the bulk Si component.

contrast corresponds to the Ni $3p$ intensity and indicates lateral variations of the Ni surface and near-surface concentration. The map evidences the presence of two types of islands with different shapes and Ni content. The ''longer'' islands contain less Ni and are always oriented in the $\langle 110 \rangle$ direction. The Ni-rich islands show a less pronounced anisotropy of the shape. The islands distinguished by SPEM cover about 4% of the surface. Simple calculations, assuming that for the present formation conditions the Ni coverage on the areas away from the islands cannot exceed 0.14 ML (the maximum coverage corresponding to close-packed RC's), results in an average island's thickness of ~22 Å (~six triple Si-Ni-Si layers for $NiSi_2$). The variable contrast of the dominating areas out of the islands indicates uneven Ni distribution with a distinct depletion zone around the islands. The width of the depletion zone is comparable for almost all islands. As can be seen from the profile linescans (averaged over the indicated by the dashed line area) it expands up to ~3 μm from the edge of the islands. SEM measurements of the sample, performed afterwards, also revealed the presence of nanosized islands with varying density, nonresolvable with SPEM.

The Si $2p$, valence band (VB) and Ni $3p$ spectra (see Fig. 2 and Table I) taken from different areas of this morphologically complex surface reveal distinctive differences in chemical interactions and electronic structures. The decomposition of all Si $2p$ spectra in Fig. 2 requires at least three spin-orbit split components after subtraction of the background.

Even without line-shape analyses the Si $2p$ and the VB spectra in Figs. 2(a)–2(c) clearly manifest the different composition of the two types of islands. The VB spectra taken from the islands reproduce well those reported for $NiSi_2$ [Figs. 2(a) and 2(b)] and NiSi samples [Fig. 2(c)].[9–11] The most intense features are due to the shifted Ni $3d$ bonding and nonbonding levels. These are for NiSi the unresolved double peak structure at ~ -1.8 and ~ -2.7 eV in Fig. 2(c) and a shoulder at Fermi edge, and for $NiSi_2$ a peak at ~ -3.1 eV in Figs. 2(a) and 2(b) with a less pronounced shoulder at the Fermi edge. Out of the islands, Figs. 2(d) and 2(e), the weight of the Ni d states decreases and accounts for the reduced intensity of the VB spectra where the relative contribution of the Si s and p states is enhanced. It should be noted that the VB spectra from both darker (d) and brighter (e) out-of-island areas resemble those of the $NiSi_2$ islands, whereas the VB spectrum of the depletion zone (f) better resembles that of Si.

TABLE I. Columns 1–3 show the BE shifts in eV with respect to the bulk Si $2p$ line for the reacted, $\Delta E_b(r)$, and ''surface,'' $\Delta E_b(s)$, components of the Si $2p$ spectra and the BE shift of Ni $3p$ levels, ΔE_b(Ni), with respect to metal Ni. The error is ± 0.1 eV. Columns 4 and 5 show the relative weight of the reacted Si $2p$ component, $I(r)/I$(total), and the normalized Ni $3p$ intensity, $I_{\mathrm{Ni}}/I_{\mathrm{Si}}$. The values are evaluated from PE spectra taken from at least three islands of the same type and different depletion zones (DZ).

PHASE	$\Delta E_b(r)$	$\Delta E_b(s)$	ΔE_b(Ni)	$I(r)/I$(tot)	$I_{\mathrm{Ni}}/I_{\mathrm{Si}}$
$NiSi_2$	−0.4	+0.3	−0.8	0.5±0.05	0.75±0.1
NiSi	−0.05	+0.5	−0.5	0.72	2.5
DZ	−0.3	+0.4	−0.65	0.25	0.08

The Si $2p$ spectra of the $NiSi_2$ islands are best fitted using one bulk Si component and a second shifted by $\sim +0.3$ eV, with respect to the bulk for the lower BE side of the Si $2p$ spectra from a third component, shifted by ~ -0.4 eV, relative to the bulk Si, for the higher BE side. The third component is broader and asymmetric and its energy position is consistent with that reported for reacted Si in the disilicide phase.[12,14] The presence of bulk Si is also in accord with previous PE studies of the $NiSi_2$ phase. It was attributed to segregation of Si on top of $NiSi_2$ and formation of an epitaxial Si layer, a process favored by the lower surface energy of Si than that of $NiSi_2$.[14,15] We tentatively assign the lowest BE component to a surface component.[13] It might correspond to the Si adatoms forming the observed STM (2×2) structure on top of the $NiSi_2$ phase.[16,17] The weight of the bulk and surface Si contributions varies with the size of the $NiSi_2$ islands; smaller islands contain a thicker Si cap, as evidenced by the spectra in Fig. 2(b). Using the known exponential dependence of the PE emission on the electron escape depth (4.2 Å for the Si $2p$ photoelectrons in our experimental setup) we evaluated from the intensities of the surface and bulk Si components surface Si atoms coverage between 0.2–0.45 ML and thickness of the Si epitaxial layer below from ~ 1 to 2 ML. It is notable that the surface atom density evaluated here is comparable with the average Si adatom density measured for the ''1×1''-RC phase, 0.39 ML.[5] The width of the silicide component implies the presence of unresolved subcomponents representing the difference of the Si environments in the three top layers of the $NiSi_2$, where Si atoms have less than four Ni neighbors.

The energy position and the weight of the fitting components for the Si $2p$ spectra of the NiSi islands [see Fig. 2(c)] are completely different: one dominant asymmetric silicide component which appears at almost the same energy as bulk Si and two weaker components shifted by +0.3 and +0.5 eV, respectively. The negligible shift (~ -0.05 eV) of the reacted component of the NiSi phase can be attributed to the larger final state relaxation in Ni-rich silicides which show high density of states at the Fermi edge. As can be seen from Table I, in contrast to $NiSi_2$, the weight of the reacted component remains the same for all NiSi islands. The origin of the other two components is not clear. The weaker one, shifted by +0.5 eV results in a small shoulder on the lower energy tail and might be ascribed to Si surface atoms. Its intensity corresponds to ~ 0.15 ML. Assuming a Si terminating plane of NiSi islands we can assign the component shifted by +0.3 eV to the top Si layer. This is in fair agreement with the intensity of this component which corresponds to ~ 0.9 ML.

It is notable that the same components used for the $NiSi_2$ islands fit well the Si spectra from the darker and brighter areas away from the islands displayed in Figs. 2(d) and 2(e). The only difference is that the weight of the ''reacted'' component is smaller, as can be seen in Table I. This $NiSi_2$-like structure is in excellent agreement with the corresponding VB spectra. These PE data are in accord with the post-SEM measurements revealing that the nanosized islands with varying density are $NiSi_2$-type, probably separated by a ''1×1''-RC surface.

The Si $2p$ spectra from the depletion zone, Fig. 2(f), where the amount of Ni is negligibly small, require components very similar to the ones used for fitting a ''1×1''-RC surface phase, obtained in a separate experiment.[9] In the ''1×1'' phase, Ni sits in a substitutional site in the top layer of the Si bilayer and is surrounded above by six Si atoms, which results in a distorted fluoritelike structure.[5] Note that the components shifted by −0.3 and +0.4 eV in this case indicate a local structure similar to that of $NiSi_2$.

The binding energy shifts of the Ni $3p$ levels, with respect to the Ni $2p$ levels of a pure Ni film (deposited on the Ta clips supporting the Si sample) for the different phases and the Ni $3p$ intensity variations, normalized against the corresponding Si $2p$ intensity, are summarized in Table I. For all phases, Ni $3p$ levels shift toward the higher BE, the amount of the shift increasing in the following order: NiSi islands; depletion zone; $NiSi_2$ islands. This trend is mainly determined by the local bonding configuration, e.g., number and distances of the nearest neighbors. It is notable that the difference in the Ni $3p$ binding energy for the NiSi and $NiSi_2$ islands, ~ 0.3 eV, is much less than that reported for orthorhombic NiSi and cubic fluoritetype $NiSi_2$ compounds, 1.6 eV, where the Ni $3p$ of the NiSi compound does not show any chemical shift with respect to metallic Ni.[12] This indicates that ''our'' NiSi islands are not identical to the orthorhombic NiSi compound. The normalized Ni $3p$ intensity values are consistent with the absence of an out-diffused Si cap on top of the NiSi islands, which attenuates the Ni $3p$ signal from the $NiSi_2$ islands.

The present results reveal new aspects of the processes involved in the formation of Ni silicide phases. We provide indisputable experimental evidence that in addition to $NiSi_2$, a second stable silicide phase, with composition and electronic structure close to NiSi, is formed during bulk-to-surface Ni segregation. The almost equal number of the two types of micron-sized islands indicates that the generally accepted sequence of reactions, where at formation temperatures above 1000 K $NiSi_2$ should be the only three-dimensional phase, is not valid, at least for the cases of low Ni coverages when island structures are created. Note that the present growth procedure is fundamentally different from SPE where metal films deposited at low temperatures are reacted by subsequent heating and the reaction starts at the Ni/Si interface. Here, *the precipitating Ni atoms are in a pure Si environment*, so that the formation of phases different from Ni-containing surface phases and $NiSi_2$ islands is even more unlikely. The coexistence of a second NiSi-like

phase supports some earlier assumptions for formation of a metastable NiSi phase with an excellent lattice match to the Si substrate[1] and the recent transmission electron microscopy/x-ray diffraction (TEM/XRD) characterization of formation stages of $NiSi_2$, pointing towards the existence of a fluorite-based NiSi phase, which is believed to be a transition phase towards the formation of an equilibrium $NiSi_2$ phase.[18]

The present results suggest the following scenario for phase formation when Ni precipitates from the bulk. NiSi islands, which obey diffusion-limited kinetics,[1] nucleate first, dragging Ni from the adjacent vicinity and resulting in a depletion zone around the islands. The width of the depletion zone can be used as a measure for the length of the Ni surface (or subsurface) diffusion during the quench which turns out to be of the order of a few microns in the present case. Despite the high temperature, only a part of the formed NiSi islands convert into $NiSi_2$, which is a nucleation-limited process.[1] The nucleation of $NiSi_2$ islands requires a sufficient number of mobile Si adatoms, because obviously Ni atoms can diffuse through the Si structure without affecting it. The directional orientation and the shape of the identified $NiSi_2$ islands supposes anisotropy of the nucleation barrier, most likely determined by anisotropy in the mass transport of Si participating in disilicide formation. The present data indicate an enhanced Si adatom density and/or higher mobility along steps or structural irregularities with edges aligned with $\langle 110 \rangle$ direction. The composition of the NiSi islands where a distinctive feature is the much thinner Si cap also supports this scenario.

In conclusion, we have shown that photoelectron spectromicroscopy analysis of phases occurring in the initial stages of development of the Ni/Si(111) system revealed uncertainty in the commonly accepted formation schemes when the phase obeys nucleation-limited kinetics. The identified islands with a NiSi stoichiometry at conditions when only Ni-containing surface phases ($\sqrt{19}$ or ''1×1'') and $NiSi_2$ islands are expected to form, demonstrate the importance of chemical analysis in determining the exact nature of the coexisting phases on morphologically complex interfaces. Considering the fact that the fluorite structure allows a significant amount of Si deficiency, we believe that this NiSi phase is structurally similar to the $NiSi_2$, which explains why it has not been distinguished by means of structure characterization methods.

These unexpected findings stimulated further photoelectron spectromicroscopy investigations on other similar interfaces produced by reactive or solid-state epitaxy. These studies are underway and also reveal peculiarities in the interface evolution.

This work was supported by an EC grant under Contract No. ERBCHGECT920013 and by Sincrotrone Trieste SCpA.

*Present address: Institute of Surface Engineering and Optoelectronics, Teslova 30, Ljubljana, Slovenia.

[1] H. von Kanel, Mater. Sci. Rep. **8**, 193 (1992).
[2] M. Y. Lee and P. A. Bennett, Phys. Rev. Lett. **75**, 4460 (1995).
[3] S. A. Parikh, M. Y. Lee, and P. A. Bennett, J. Vac. Sci. Technol. A **13**, 1589 (1995); Surf. Sci. **356**, 53 (1996).
[4] M. Yoshimura, S. Shinabe, and T. Yao, Surf. Sci. **357**, 917 (1996).
[5] P. A. Bennett *et al.*, J. Vac. Sci. Technol. A **13**, 1728 (1995).
[6] A. E. Dolbak *et al.*, Surf. Sci. **247**, 32 (1991).
[7] M. Marsi *et al.*, J. Electron Spectrosc. Relat. Phenom. **84**, 73 (1997).
[8] S. Günther *et al.*, Phys. Rev. B **56**, 5003 (1997).
[9] L. Gregoratti *et al.* (unpublished).
[10] W. Speier *et al.*, Phys. Rev. B **39**, 6008 (1989).
[11] D. D. Sarma *et al.*, J. Phys.: Condens. Matter **1**, 9131 (1989).
[12] A. Franciosi, J. M. Weaver, and F. A. Schmidt, Phys. Rev. B **26**, 546 (1982).
[13] F. J. Himpsel *et al.*, in *Core Level Spectroscopy of Silicon Surfaces and Interfaces*, Proceedings of the International School of Physics ''Enrico Fermi,'' Course CVIII, Varenna, 1988, edited by M. Campagna and R. Rosei (Elsevier, City, 1990), p. 203.
[14] V. Hinkel *et al.*, Appl. Phys. Lett. **50**, 1257 (1987).
[15] A. R. Miedema, Z. Metallkd. **69**, 287 (1978); **69**, 455 (1978).
[16] T. Jao, Sh. Shinabe, and M. Yoshirima, Appl. Surf. Sci. **104**, 213 (1996).
[17] P. A. Bennett, S. A. Parikh, M. Y. Lee, and D. G. Cahill, Surf. Sci. **312**, 377 (1994).
[18] H. L. Ho *et al.*, J. Mater. Res. **11**, 904 (1996).